NORDITA-2000/20 HE
LU TP 00-09
DAPNIA/SPHN-00-11
hep-ph/0003257
March 27, 2000

arXiv:hep-ph/0003257 27 Mar 2000

Semi-Exclusive Production of Photons at HERA

Paul Hoyer

NORDITA
Blegdamsvej 17, 2100 Copenhagen, Denmark

Martin Maul

Department of Theoretical Physics, Lund University
Sölvegatan 14 a, S-223 62 Lund, Sweden

Andreas Metz

DAPNIA/SPhN, CEA-Saclay
F-91191 Gif-sur-Yvette, France

We study the feasibility of measuring semi-exclusive photon production $\gamma + p \to \gamma + Y$ at HERA. The cross section of photons produced at large transverse momenta, recoiling off an inclusive system Y of limited mass, can without photon isolation cuts be simply expressed in terms of hard pQCD subprocesses and standard target parton distributions. With the help of event generators we identify the kinematic region where quark and gluon fragmentation processes can be neglected. The cross section in this semi-exclusive region is large enough to be measured with an upgraded HERA luminosity of $\mathcal{L} = 100\,\mathrm{pb}^{-1}$.

The subprocesses of lowest order in α_s are suppressed at low recoil masses M_Y, compared to higher order gluon exchange, i.e. BFKL contributions. The distinct M_Y-dependence makes it possible to determine experimentally the kinematic range where the higher order processes dominate.

PACS: 12.38.-t, 13.60.-r, 14.70.Bh
Keywords: semi-exclusive reactions, photoproduction, Monte Carlo simulation.

I. INTRODUCTION

Semi-exclusive reactions of the type $A + B \to C + Y$, where particle C emerges with large transverse momentum and the mass of the inclusive system Y satisfies $\Lambda_{QCD} \ll M_Y \ll E_{cm}$, provide a new tool for probing the structure of hadrons [1]. It is analogous to DIS, $ep \to eX$, in the sense that particles A and C form an effective current which probes the target B at large momentum transfer $t = (p_A - p_C)^2$, producing the inclusive system Y. Semi-exclusive cross sections factorize into a calculable short distance interaction times a standard target parton (b) distribution $f_{b/B}(x_S, -t)$ according to

$$\frac{d\sigma}{dt\, dx_S}(A + B \to C + Y) = \sum_b f_{b/B}(x_S, -t) \frac{d\sigma}{dt}(Ab \to Cd) , \tag{1}$$

where

$$x_s = -t/(M_Y^2 - t) \tag{2}$$

and the momentum transfer $-t$ serves as factorization scale. For large $-t$ only compact configurations of particles A and C participate in the reaction, and their re-interactions with the target are suppressed. The final parton(s) d merges with the target spectators to form the inclusive system Y.

In this paper we discuss the feasibility of measuring the semi-exclusive process $\gamma p \to \gamma Y$ (Fig. 1) at HERA. This process is particularly favorable since photons have a point like component which is selected by the semi-exclusive dynamics. The lowest order pQCD subprocesses are shown in Fig. 2a,b.

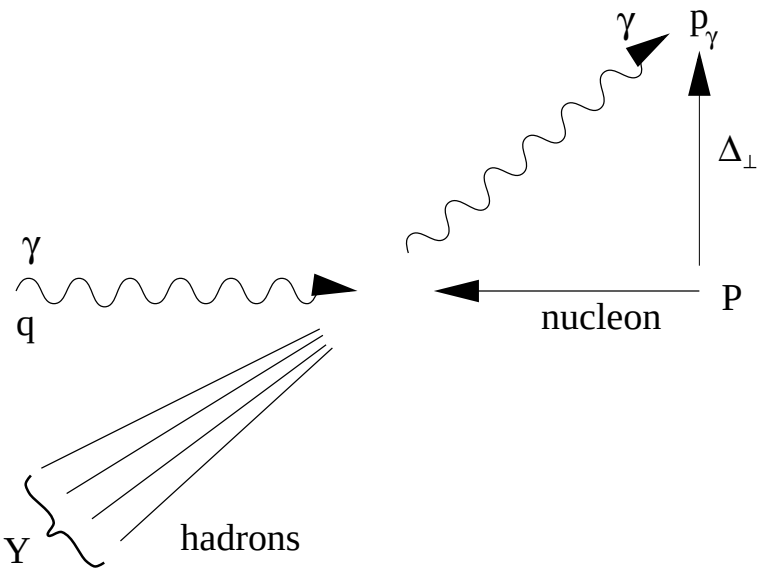

FIG. 1. Kinematics of the semi-exclusive photoproduction of photons.

HERA data on photon production at large transverse momentum have previously been studied [2–6] in terms of an isolation cut, which ensures low accompanying transverse energy in a cone around the photon direction. Such a cut removes a large fraction of the photons produced by fragmentation and decay, but allows 'resolved' photon contributions, where a photon remnant emerges at low transverse momentum. In a semi-exclusive process particles in the incoming and outgoing photon directions are kinematically prohibited by the condition $M_Y^2 = (P + q - p_\gamma)^2 \ll W^2$, where $W^2 = (q + P)^2$ is the total E_{CM}^2 of the γp system. The price paid in cross section is rewarded by model independence of the theoretical analysis. In particular, there are no contributions from parton fragmentation, hadron decay nor resolved photon processes.

In practice some model dependence is introduced through the estimate of what restrictions on t and M_Y^2 must be imposed in order to eliminate backgrounds from competing processes. We use the PYTHIA [7] and LUCIFER

[8] Monte Carlo generators to model photon production via fragmentation and hadron decay, and find that these processes do not contribute for $W^2/M_Y^2 \gtrsim 10$ and $-t \gtrsim 4$ GeV^2. We also estimate that for incoming photon virtualities $Q^2 \lesssim 0.1$ GeV^2 photon emission from the electron line (the Bethe-Heitler process) is insignificant.

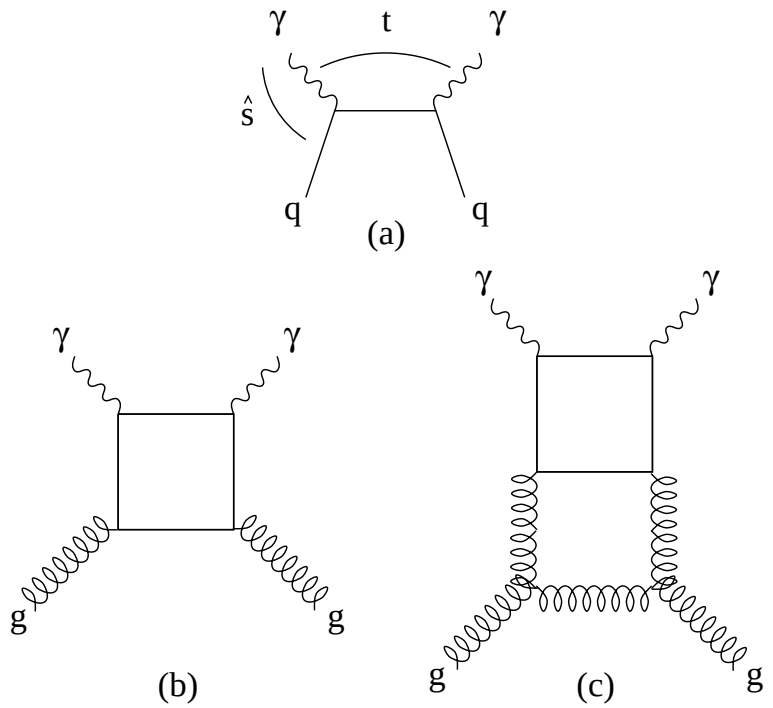

FIG. 2. Compton scattering subprocesses: Low order scattering on a quark (a) and on a gluon (b). At high $\hat{s}/-t$, higher order amplitudes like (c) dominate, due to gluon exchange in the t-channel.

It is important to notice that the low order pQCD amplitudes of Fig. 2a,b actually are suppressed at high subenergies $\hat{s} = x_s W^2$. These amplitudes are $\propto \hat{s}^0$, whereas the higher order amplitude of Fig. 2c is $\propto \hat{s}^1$ due to two gluon exchange in the t-channel. At even higher orders repeated gluon ladders are expected to build up hard Pomeron exchange in the BFKL approximation, as has been studied extensively for the present process [9–12]. It is worthwhile to explore at what value of $\hat{s}/-t$ the higher order diagrams begin to dominate. We find that the BFKL amplitude is numerically important compared to the lowest order contributions in the whole semi-exclusive range $\hat{s}/-t \gtrsim 10$. If the BFKL approximation is reliable (or the amplitude of Fig. 2c dominates) at such moderate values of the subprocess energy then the subprocess cross section will be found to grow (or be constant) in this whole range. Alternatively, if the lowest order diagrams dominate, the subprocess cross section will decrease in the lower range of $\hat{s}/-t$. This would make it smaller than the BFKL estimate at high $\hat{s}/-t$.

II. SUBPROCESS CROSS SECTIONS

The lowest order cross section for $\gamma q \to \gamma q$ (Fig. 2a) is [13]

$$\frac{d\sigma_{\rm LO}}{dt}(\gamma q \to \gamma q) = \frac{2\pi e_q^4 \alpha^2}{\hat{s}^2}\left(\frac{\hat{s}}{-\hat{u}} + \frac{-\hat{u}}{\hat{s}}\right), \tag{3}$$

with $\alpha = e^2/4\pi$. For the lowest order $\gamma g \to \gamma g$ process (Fig. 2b) we have analogously [14,15],

$$\frac{d\sigma_{\rm LO}}{dt}(\gamma g \to \gamma g) = 2\left(\sum_q e_q^2\right)^2 \frac{\alpha^2 \alpha_s^2}{64\pi \hat{s}^2}\left[|M_1(\hat{s},t,\hat{u})|^2 + |M_1'(\hat{u},t,\hat{s})|^2 + |M_1'(t,\hat{s},\hat{u})|^2 + 20\right], \tag{4}$$

where

$$|M_1(\hat{s},t,\hat{u})|^2 = \left(2+2\frac{t-\hat{u}}{\hat{s}}\ln\frac{t}{\hat{u}}+\frac{t^2+\hat{u}^2}{\hat{s}^2}\left[\ln^2\frac{t}{\hat{u}}+\pi^2\right]\right)^2 ,$$
$$|M_1'(\hat{u},t,\hat{s})|^2 = \left(2+2\frac{\hat{s}-t}{\hat{u}}\ln\frac{\hat{s}}{-t}+\frac{\hat{s}^2+t^2}{\hat{u}^2}\ln^2\frac{\hat{s}}{-t}\right)^2+4\pi^2\left(\frac{\hat{s}^2+t^2}{\hat{u}^2}\ln\frac{\hat{s}}{-t}+\frac{\hat{s}-t}{\hat{u}}\right)^2 . \quad (5)$$

It is interesting to compare the size of the BFKL cross section to the LO ones given above. The $\gamma g \to \gamma g$ BFKL cross section is to leading logarithmic accuracy given by [10–12]

$$\frac{d\sigma_{\rm BFKL}}{dt}(\gamma g\to\gamma g) = \frac{81}{16}\frac{\alpha^2\alpha_s^4}{576t^2}\pi\left(\sum_q e_q^2\right)^2\left[G\left(\frac{3\alpha_s}{\pi}\ln\frac{\hat{s}}{-t}\right)\right]^2, \quad \text{with}$$
$$G(z) = \int_{-\infty}^{\infty}\frac{d\nu}{1+\nu^2}\frac{\nu^2}{\left(\nu^2+\frac{1}{4}\right)^2}\frac{\tanh(\pi\nu)}{\pi\nu}2(11+12\nu^2)\exp\left[z\chi(\nu)\right] ,$$
$$\chi(\nu) = 2\psi(1)-2{\rm Re}\left[\psi\left(\frac{1}{2}+i\nu\right)\right] . \quad (6)$$

In Fig. 3 we show the dimensionless lowest order cross sections $\hat{s}^2 d\sigma/dt$ for $\gamma u \to \gamma u$ (solid line) and $\gamma g \to \gamma g$ (times 10, dot-dashed line). The small size of the lowest order $\gamma g \to \gamma g$ cross section means that it will be insignificant also in the physical process $\gamma N \to \gamma Y$, even though the gluon distribution is larger than the quark one at low values of x_s. The dashed line shows the BFKL cross section (6) for $\gamma g \to \gamma g$, based on iterating higher order diagrams like that in Fig. 2c. We used the fixed value $\alpha_s = 0.2$ indicated by BFKL fits to HERA and Tevatron data [16–18]. The BFKL cross section is comparable to the lowest order one already at $\hat{s}/-t \simeq 10$, with their ratio growing roughly as $(\hat{s}/-t)^2$. It should be stressed, however, that the BFKL analysis is expected to be reliable only for $\hat{s}/-t \gtrsim 100$ [12], and that there may be sizeable corrections from NLO corrections [19].

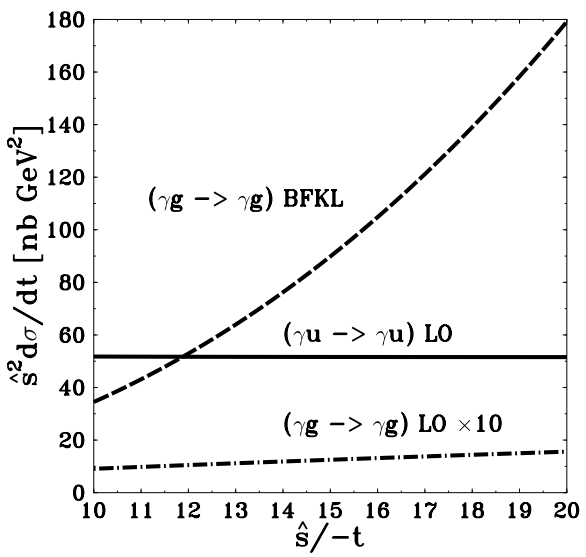

FIG. 3. Lowest order subprocess cross sections $\hat{s}^2 d\sigma/dt$ for $\gamma u \to \gamma u$ (solid line) and $\gamma g \to \gamma g$ (times 10, dot-dashed line) for $10 \le \hat{s}/-t \le 20$. The dashed line shows the BFKL cross section extrapolated to this region of moderate subprocess energy, assuming $\alpha_s = 0.2$. Three active flavors have been used in both the calculation of the process $\gamma g \to \gamma g$ to LO and the BFKL contribution.

III. SEMI-EXCLUSIVE PHOTON ELECTROPRODUCTION AT HERA

The $ep \to e\gamma Y$ electroproduction cross section is in the semi-exclusive limit $\Lambda^2_{QCD} \ll -t, M_Y^2 \ll W^2$ related to the subprocesses through

$$\frac{d\sigma}{dy\,dt\,dx_s}(ep \to e\gamma Y) = f_{\gamma/e}(y, Q^2_{\max}) \sum_{i \in q,g} f_{i/p}(x_s, -t) \frac{d\sigma}{dt}(\gamma i \to \gamma i)\,. \tag{7}$$

Here y is the fraction of momentum that the photon, of virtuality $\leq Q^2_{\max}$, takes of the electron beam. The Weizsäcker-Williams function $f_{\gamma/e}(y, Q^2_{\max})$ is given in [20],

$$f_{\gamma/e}(y, Q^2_{\max}) = \frac{\alpha}{2\pi}\left[\frac{(1+(1-y)^2)}{y} \ln \frac{Q^2_{\max}(1-y)}{m_e^2 y^2} + 2m_e^2 y \left(\frac{1}{Q^2_{\max}} - \frac{1-y}{m_e^2 y^2}\right)\right]. \tag{8}$$

In our kinematical range the Weizsäcker-Williams scale is identical to the upper limit of the photon virtuality Q^2_{max}, as the typical hard scale $-t$, which characterizes the production process, is much larger than Q^2_{max}. A detailed discussion of the choice of the Weizsäcker-Williams scale can be found in Refs. [20,21]. For the parton distributions $f_{i/p}(x_s, -t)$ we use the GRV94 LO parameterizations [22].

In this section we first estimate the kinematic region in which the semi-exclusive production mechanism dominates, and then evaluate the physical cross section in this region.

A. Background from Fragmentation and Decay in Photoproduction

Large transverse momentum photons can be produced through quark and gluon fragmentation $q, g \to \gamma + X$, following standard hard scattering processes such as photon gluon fusion $\gamma g \to q\bar{q}$ and gluon bremsstrahlung $\gamma q \to qg$. A second source of contributions are photons from hadronic decays like $\pi^0 \to \gamma\gamma$. In the following we call both background contributions 'fragmentation'. Such processes typically give hadrons in the photon direction, and are thus suppressed in the limit where $M_Y^2 \ll W^2$.

We have used the Monte Carlo event generators PYTHIA [7] and LUCIFER [8] to estimate the range of W^2/M_Y^2 in which semi-exclusive production dominates over fragmentation. These event generators include the direct (semi-exclusive) $\gamma q \to \gamma q$ cross section only at lowest order. The true semi-exclusive cross section may be larger than simulated, due to the neglect of higher order (BFKL) contributions. Hence our estimate of the significance of the fragmentation background is expected to be conservative. We do not consider possibilities to reduce the fragmentation contribution using photon isolation cuts [2–6].

We evaluate the contributions from the direct process $\gamma q \to \gamma q$ and that from the background $\gamma g \to q\bar{q}$ and $\gamma q \to qg$ processes separately. If the final state contains several photons, we choose the one with largest energy E_γ^{CM} in the CM frame of the photon and the nucleon. The invariant mass M_Y^2 of the remaining particles is then given by $M_Y^2 = W^2 - 2WE_\gamma^{CM}$.

In Fig. 4 we show the PYTHIA and LUCIFER results for $W = 200$ GeV and two ranges of photon transverse momentum, 4 GeV$^2 < -t < 10$ GeV^2 and 10 GeV$^2 < -t < 30$ GeV^2. It may be seen that the semi-exclusive process $\gamma q \to \gamma q$ starts to dominate for $W^2/M_Y^2 \gtrsim 10$. We have checked that the same conclusion holds for $W = 80$ GeV. Note that for $M_Y^2 \gg -t$, the subprocess variable $\hat{s}/-t$ of Fig. 3 is in the semi-exclusive limit simply related to W^2/M_Y^2,

$$\frac{W^2}{M_Y^2} = \frac{\hat{s}}{-t}\left(1 - \frac{t}{M_Y^2}\right) \simeq \frac{\hat{s}}{-t}\,. \tag{9}$$

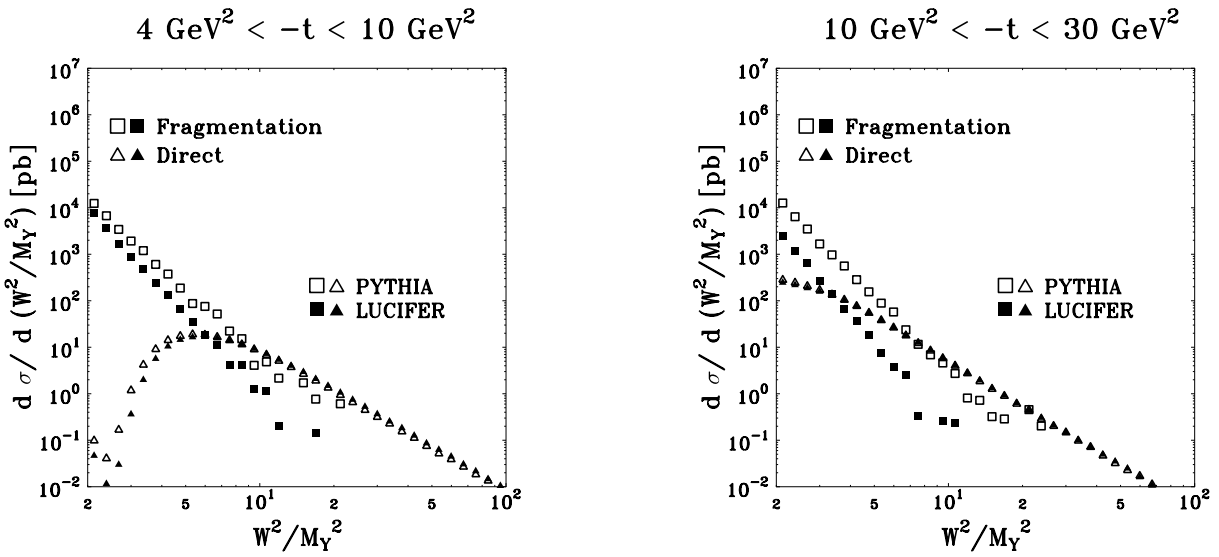

FIG. 4. Inclusive cross sections $d\sigma(\gamma p \to \gamma Y)/d(W^2/M_Y^2)$ for the photon with the largest E_γ^{CM} per event at $W = 200$ GeV. The t-range is 4 GeV^2 $< -t <$ 10 GeV^2 (left), and 10 GeV^2 $< -t <$ 30 GeV^2 (right). The triangles show the direct ($\gamma q \to \gamma q$) contribution of Eq. (3) and the squares show photons generated by fragmentation. The open squares and triangles are the result of the PYTHIA program and the filled squares and triangles are from the LUCIFER run. An additional cut $.001 < x_s < .7$ has been applied in both figures. Higher order parton showering and resolved photon contributions are not included.

B. Background from the Bethe-Heitler Process in Electroproduction

When the incoming photon has virtuality $Q^2 \neq 0$ the final photon may be radiated off the electron (the Bethe-Heitler (BH) process, see Fig. 5 a). We wish to determine the maximum value of Q^2 for which the BH cross section can be neglected compared to that of photon emission from the quark (Virtual Compton Scattering (VCS), see Fig. 5 b).

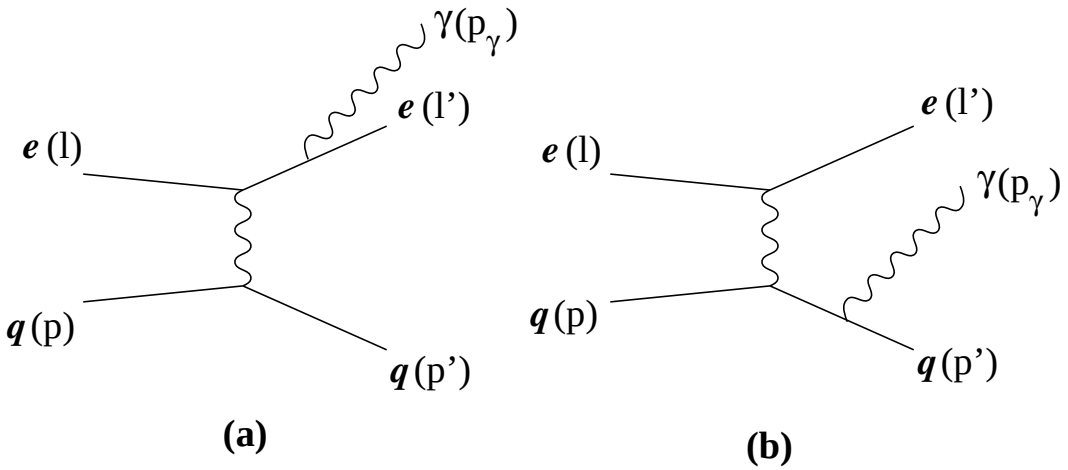

FIG. 5. Sample diagrams for photon production via the Bethe-Heitler (BH) process (a) and Virtual Compton Scattering (VCS) (b).

At finite Q^2 the lowest order $ep \to e\gamma Y$ cross section can be written

$$\frac{d\sigma_{LO}(ep\to e\gamma Y)}{dx_s\,dW^2\,dQ^2\,dt\,d\phi}=\frac{1}{2(4\pi)^4x_sW_{ep}^4(\hat{s}+Q^2)}\sum_q f_{q/p}(x_s,-t)\overline{|\mathcal{M}_q|^2}\,,\quad\text{with} \tag{10}$$

$$\overline{|\mathcal{M}_q|^2}=\overline{|\mathcal{M}_q^{VCS}|^2}+\overline{|\mathcal{M}_q^{BH}|^2}+\overline{2\mathrm{Re}\left(\mathcal{M}_q^{BH}\mathcal{M}_q^{VCS\,*}\right)}\,.$$

Here $Q^2=-q^2=-(l-l')^2$ and $\hat{s}=(q+p)^2=x_sW_{\gamma p}^2$ in the notation of Fig. 5. ϕ is the angle between $\vec{q}\times\vec{p}_\gamma$ and $\vec{\ell}\times\vec{\ell}'$ with the three-vectors given in the CM frame of the virtual photon and the proton, while $W_{ep}\approx 300$ GeV is the ep CM energy. We also define

$$\hat{s}_l=(l'+p_\gamma)^2\,,\quad \hat{u}_l=(l-p_\gamma)^2 \tag{11}$$

which can be obtained from $\hat{s}$ and $\hat{u}$ by replacing the quark momentum $p(p')$ with the lepton momentum $l(l')$.

The squared VCS and BH matrix elements can now be written as

$$\overline{|\mathcal{M}_q^{VCS}|^2}=\frac{-4(4\pi\alpha)^3e_q^4}{Q^2\hat{s}\hat{u}}F\,, \tag{12}$$

$$\overline{|\mathcal{M}_q^{BH}|^2}=\frac{4(4\pi\alpha)^3e_q^2}{t\hat{s}_l\hat{u}_l}F\,, \tag{13}$$

with the common factor F given by

$$F=\hat{s}^2+(\hat{s}+t)^2+\hat{u}_l^2+(2W_{eq}^2+\hat{u}_l)^2-2\hat{s}(2W_{eq}^2+\hat{u}_l)-2t(W_{eq}^2+\hat{u}_l)+2Q^2(2\hat{s}+t-3W_{eq}^2-2\hat{u}_l)+3Q^4\,, \tag{14}$$

and $W_{eq}^2=(l+p)^2=x_sW_{ep}^2$.

The expression for the interference term can be given in a symmetric form,

$$\begin{aligned}\overline{2\mathrm{Re}\left(\mathcal{M}_q^{BH}\mathcal{M}_q^{VCS\,*}\right)}=\frac{8(4\pi\alpha)^3e_q^3}{Q^2t}\Bigg\{&Q^2\left[-\frac{1}{2}(\hat{s}-\hat{u})\left(\frac{1}{\hat{s}_l}-\frac{1}{\hat{u}_l}\right)+\frac{1}{\hat{u}_l}(l\cdot p+l\cdot p')+\frac{1}{\hat{s}_l}(l'\cdot p+l'\cdot p')\right]\\
&+t\left[\frac{1}{2}(\hat{s}_l-\hat{u}_l)\left(\frac{1}{\hat{s}}-\frac{1}{\hat{u}}\right)-\frac{1}{\hat{u}}(l\cdot p+l'\cdot p)-\frac{1}{\hat{s}}(l\cdot p'+l'\cdot p')\right]\\
&-8(l\cdot p\,l'\cdot p'+l\cdot p'\,l'\cdot p)\left(\frac{l\cdot p}{\hat{u}\hat{u}_l}+\frac{l\cdot p'}{\hat{s}\hat{u}_l}+\frac{l'\cdot p}{\hat{u}\hat{s}_l}+\frac{l'\cdot p'}{\hat{s}\hat{s}_l}\right)\\
&+l\cdot p\left[\frac{\hat{s}\hat{s}_l}{\hat{u}\hat{u}_l}-3+\frac{2}{\hat{u}\hat{u}_l}\left(\hat{s}l'\cdot p+\hat{s}_l l\cdot p'-(\hat{u}+\hat{u}_l)l'\cdot p'\right)\right]\\
&+l\cdot p'\left[\frac{\hat{u}\hat{s}_l}{\hat{s}\hat{u}_l}-3+\frac{2}{\hat{s}\hat{u}_l}\left(-\hat{s}_l l\cdot p-\hat{u}l'\cdot p'+(\hat{s}+\hat{u}_l)l'\cdot p\right)\right]\\
&+l'\cdot p\left[\frac{\hat{s}\hat{u}_l}{\hat{u}\hat{s}_l}-3+\frac{2}{\hat{u}\hat{s}_l}\left(-\hat{s}l\cdot p-\hat{u}_l l'\cdot p'+(\hat{u}+\hat{s}_l)l\cdot p'\right)\right]\\
&+l'\cdot p'\left[\frac{\hat{u}\hat{u}_l}{\hat{s}\hat{s}_l}-3+\frac{2}{\hat{s}\hat{s}_l}\left(\hat{u}l\cdot p'+\hat{u}_l l'\cdot p-(\hat{s}+\hat{s}_l)l\cdot p\right)\right]\Bigg\}.\end{aligned} \tag{15}$$

In Fig. 6 we compare the VCS to the total VCS+BH cross section for $ep\to e\gamma Y$ as a function of $Q^2_{\max}$, the maximum photon virtuality. The differential cross section (10) was integrated over the ranges $x_s\in[0.01,0.7]$, $W\in[40\text{ GeV},160\text{ GeV}]$, $\phi\in[0,2\pi]$, $-t\in[4\text{ GeV}^2,10\text{ GeV}^2]$, and $Q^2\in[m_e^2,Q^2_{\max}]^*$.

---

*In order to ensure that the electron propagators are far off-shell we also required $\hat{s}_l,-\hat{u}_l>-t_{\min}=4$ GeV^2. This cut is, however, irrelevant for $Q^2\lesssim 1$ GeV^2.

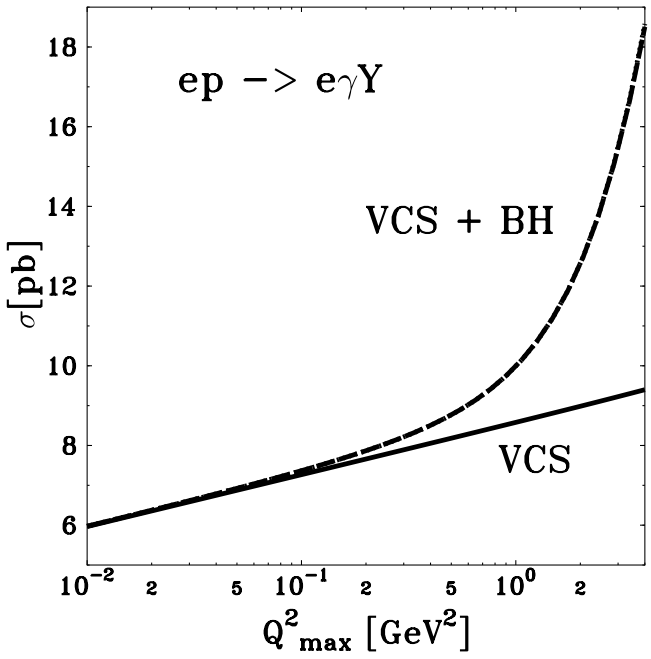

FIG. 6. Dependence of the total $ep \to e\gamma Y$ cross section on the maximal photon virtuality $Q^2_{\rm max}$. The solid line shows the contribution of Virtual Compton Scattering (VCS, Fig. 5b) alone, while the dashed line includes also the Bethe-Heitler (BH, Fig. 5a) contribution and the interference term. The kinematic region is defined in the text.

C. The Semi-Exclusive Cross Section

We have found that the process $ep \to e\gamma Y$ can be used to study semi-exclusive photon production at HERA in the kinematic range $W^2/M_Y^2 \gtrsim 10$, $Q^2 \lesssim 0.1$ GeV^2 and $-t \gtrsim 4$ GeV^2. In Fig. 7 we show the cross section

$$\frac{d\sigma(ep \to e\gamma Y)}{d(W^2/M_Y^2)} = \int_{0.25}^{0.75} dy f_{\gamma/e}(y, Q^2_{\rm max} = 0.1 \text{ GeV}^2) \int_{|t|_{\rm min}}^{|t|_{\rm max}} dt \frac{-t(1-x_s)^2}{W^2} \sum_{i \in q,g} f_{i/p}(x_s, -t) \frac{d\sigma}{dt}(\gamma i \to \gamma i) \qquad (16)$$

for two ranges of momentum transfer, 4 GeV^2 $< -t <$ 10 GeV^2 and 10 GeV^2 $< -t <$ 30 GeV^2. The full curve shows the contribution of the LO process of Eq. (3) (Fig. 2a). The dashed curve shows the contribution of the BFKL subprocess of Eq. (6) (Fig. 2c, plus gluon ladder iterations), together with the corresponding $\gamma q \to \gamma q$ sea quark BFKL contribution [11],

$$\frac{d\sigma_{\rm BFKL}}{dx_s dt} = \left[g(x_s, -t) + \frac{16}{81} \Sigma(x_s, -t) \right] \frac{d\sigma_{\rm BFKL}}{dt}(\gamma g \to \gamma g) \ , \qquad (17)$$

where Σ denotes the quark singlet distribution $\Sigma = \sum_q [f_{q/p} + \bar{f}_{q/p}]$. We use $\alpha_s = 0.2$ in the BFKL cross section and assume three (four) active flavors in the low (high) $|t|$-range. The horizontal dash-dotted line indicates the 1 event level per unit of W^2/M_Y^2, given a nominal HERA luminosity of 100 events/pb.

We should emphasize that the BFKL approximation may not be reliable for $W^2/M_Y^2 \lesssim 100$ [12], hence the dashed curve is an extrapolation. It is nevertheless interesting to observe that this extrapolation dominates the LO $q\gamma \to q\gamma$ contribution over the whole semi-exclusive range $W^2/M_Y^2 \gtrsim 10$. This conclusion is insensitive to the t-range and also to the range of y (not shown).

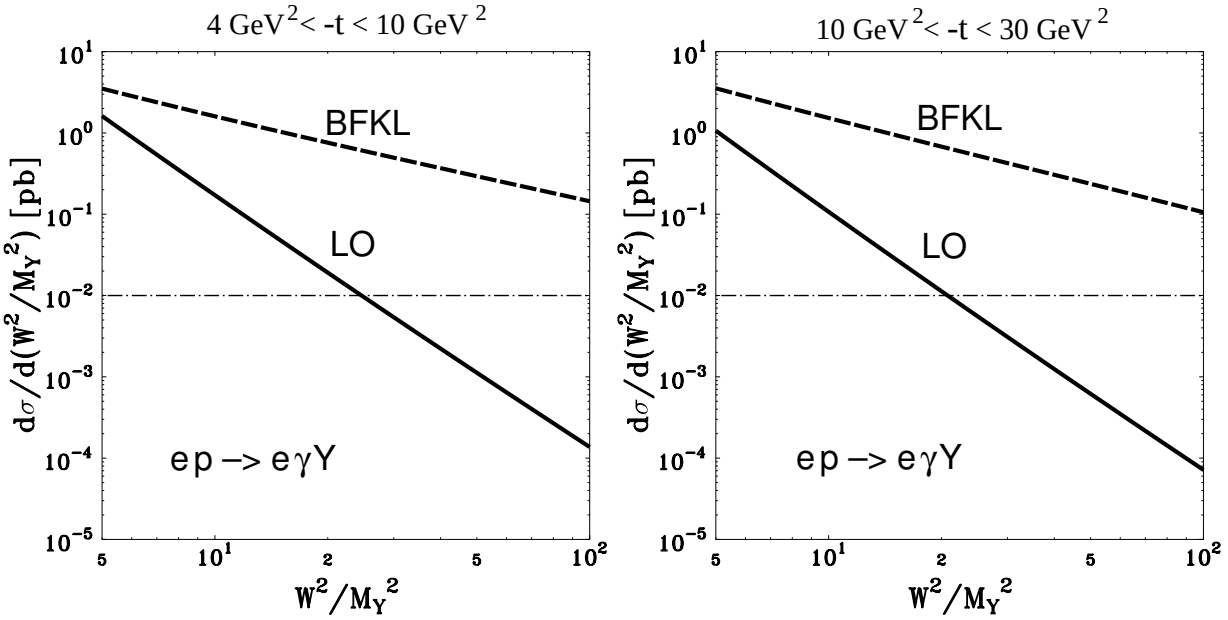

FIG. 7. The cross section $d\sigma(ep \to e\gamma Y)/d(W^2/M_Y^2)$ of Eq. (16) shown for two ranges of t: 4 GeV^2< $-t$< 10 GeV^2 (left) and 10 GeV^2 <$-t$< 30 GeV^2 (right). The solid line shows the contribution of the LO process of Eq. (3) (Fig. 2a). The dashed line shows that of the BFKL process of Eq. (17) (Fig. 2c plus gluon ladder iterations). The horizontal dash-dotted line gives the 1 event level per unit of W^2/M_Y^2, for a HERA luminosity of 100 events/pb.

IV. CONCLUSIONS

Semi-exclusive processes $A + B \to C + Y$ provide a new tool for investigating hadron structure. Effective currents formed by the $A\overline{C}$ system generalize the virtual photon probe familiar from DIS and can carry charge, flavor, baryon and other quantum numbers [1]. Before this tool can be put to use, at least two questions need to be answered:

(i) *How stringent limits* $\Lambda^2_{QCD} \ll -t, M_Y^2 \ll W^2$ *must be imposed in order for the semi-exclusive production mechanism to dominate?*
(ii) *Can the hard* $A\overline{C}$ *vertex be reliably computed using pQCD?*

In this paper we studied the process $\gamma p \to \gamma Y$, which is especially simple in the sense that both particles A and C have a point like component. Based on simulations with the PYTHIA and LUCIFER event generators we concluded that semi-exclusive dynamics should dominate for $W^2/M_Y^2 \gtrsim 10$ and $-t \gtrsim 4$ GeV^2. Photon emission from the electron (the Bethe-Heitler process) is insignificant for incoming photon virtualities $Q^2 \lesssim 0.1$ GeV^2, and can be further suppressed with angular cuts. The semi-exclusive cross section should be measurable at HERA, assuming that the subprocess cross section $\hat{\sigma}(\gamma q \to \gamma q)$ is not smaller than its lowest order (LO) pQCD approximation.

Point (ii) above is non-trivial, since the semi-exclusive kinematics implies a high energy (Regge) limit for the subprocess, $\hat{s}/-t \gg 1$. Little is known about the importance of higher order (HO) pQCD corrections in this limit. In the process under study the situation is particularly intriguing since the LO subprocess diagrams shown in Fig. 2a,b correspond to $q\bar{q}$ exchange in the t-channel. At high subenergies $\hat{s}$ they are therefore suppressed by a factor $1/\hat{s}^2$ in the cross section compared to the $\mathcal{O}(\alpha_s^4)$ gluon exchange contribution of Fig. 2c. The latter is, on the other hand, just the first term in the series of gluon ladder diagrams which is supposed to build up the BFKL Pomeron in this process [10–12].

It is not clear from which value of $\hat{s}/-t$ HO contributions like Fig. 2c start to dominate the LO processes of Fig. 2a,b. The BFKL approximation has been assumed to be relevant for $\hat{s}/-t \gtrsim 100$ [12]. Extrapolating the BFKL cross section to lower energies we found (Fig. 7) that it would in fact dominate the LO cross section in the whole range of semi-exclusive dynamics, $\hat{s}/-t \gtrsim 10$. The ratio σ_{HO}/σ_{LO} behaves approximately like $(W^2/M_Y^2)^2$, closely reflecting the $\hat{s}/-t$ dependence of the respective subprocesses, *cf.* Eq. (9). There are thus good prospects for determining the nature of the dominant t-channel exchange from experimental data.

We conclude that experimental studies of $\gamma p \to \gamma Y$ in the semi-exclusive limit will provide valuable information on the possibilities for studying hadrons using effective, 'tailored' local currents. The data will also show the importance of higher order pQCD (including BFKL) contributions to hard subprocesses at large $\hat{s}/-t$.

Acknowledgements. We are grateful for helpful discussions with Stan Brodsky and Markus Diehl. This work is supported in part by the EU/TMR contract EBR FMRX-CT96-0008.

---

[1] S.J. Brodsky, M. Diehl, P. Hoyer and S. Peigne, Phys. Lett. **B449** (1999) 306, [hep-ph/9812277].
For earlier related work, see C.E. Carlson and A.B. Wakely, Phys. Rev. **D48** (1993) 2000.
[2] J. Breitweg *et al.* (ZEUS Collaboration), Phys. Lett. **B413** (1997) 201, [hep-ex/9708038] and DESY 99-161, hep-ex/9910045.
[3] S.W. Lee, GLAS-PPE/1999-09, hep-ex/9911051.
[4] L.E. Gordon, Phys. Rev. **D57** (1998) 235, [hep-ph/9707464].
[5] M. Krawczyk and A. Zembrzuski, IFT 98/12, hep-ph/9810253.
[6] S. Frixione, Phys. Lett. **B429** (1998) 369, [hep-ph/9801442].
[7] T. Sjöstrand, Comput. Phys. Commun. **82** (1994) 74.
[8] G. Ingelman and A. Weigend, Comput. Phys. Commun. **46** (1987) 241.
[9] I. F. Ginzburg and D. Y. Ivanov, Phys. Rev. **D54** (1996) 5523 [hep-ph/9604437].
[10] D.Y. Ivanov and M. Wüsthoff, Eur. Phys. J. **C8** (1999) 107, [hep-ph/9808455].
[11] N.G. Evanson and J.R. Forshaw, Phys. Rev. **D60** (1999) 034016, [hep-ph/9902481].
[12] B.E. Cox and J.R. Forshaw, hep-ph/9912486.
[13] A. Afanasev, C.E. Carlson and C. Wahlquist, Phys. Rev. **D58** (1998) 054007, [hep-ph/9706522].
[14] M.A. Doncheski and R.W. Robinett, Phys. Rev. **D46** (1992) 2011.
[15] E.L. Berger, E. Braaten and R.D. Field, Nucl. Phys. **B239** (1984) 52.
[16] J. Bartels, J. R. Forshaw, H. Lotter and M. Wüsthoff, Phys. Lett. **B375** (1996) 301 [hep-ph/9601201].
[17] ZEUS Collaboration, *Study of the Diffractive Production of Vector Mesons at Large Q^2 or at high $|t|$ at HERA*, Contribution to the International Europhysics Conference on High Energy Physics, Tampere, Finland 1999.
See also `http://zedy00.desy.de/~schlenst/eps99_paper.html`.
[18] B. Cox, J. Forshaw and L. Lönnblad, JHEP **9910** (1999) 023 [hep-ph/9908464].
[19] V. S. Fadin and L. N. Lipatov, Phys. Lett. **B429** (1998) 127 [hep-ph/9802290].
[20] S. Frixione, M.L. Mangano, P. Nason and G. Ridolfi, Phys. Lett. **B319** (1993) 339, [hep-ph/9310350].
[21] S. Frixione and G. Ridolfi, Nucl. Phys. **B507** (1997) 315 [hep-ph/9707345].
[22] M. Glück, E. Reya and A. Vogt, Z. Phys. **C67** (1995) 433.